Dalton Transactions

RSC Publishing

PAPER

View Article Online
View Journal | View Issue

Cite this: *Dalton Trans.*, 2013, **42**, 11589

Structural and thermodynamic properties of molecular complexes of aluminum and gallium trihalides with bifunctional donor pyrazine: decisive role of Lewis acidity in 1D polymer formation†

Tatiana N. Sevastianova,[a] Michael Bodensteiner,[b] Anna S. Lisovenko,[a] Elena I. Davydova,[a] Manfred Scheer,[b] Tatiana V. Susliakova,[a] Irina S. Krasnova[a] and Alexey Y. Timoshkin*[a]

Solid state structures of group 13 metal halide complexes with pyrazine (pyz) of 2 : 1 and 1 : 1 composition have been established by X-ray structural analysis. Complexes of 2 : 1 composition adopt molecular structures $MX_3{\cdot}pyz{\cdot}MX_3$ with tetrahedral geometry of group 13 metals. Complexes of $AlBr_3$ and $GaCl_3$ of 1 : 1 composition are 1D polymers $(MX_3{\cdot}pyz)_\infty$ with trigonal bipyramidal geometry of the group 13 metal, while the weaker Lewis acid GaI_3 forms the monomeric molecular complex $GaI_3{\cdot}pyz$, which is isostructural to its pyridine analog $GaI_3{\cdot}py$. Tensimetry studies of vaporization and thermal dissociation of $AlBr_3{\cdot}pyz$ and $AlBr_3{\cdot}pyz{\cdot}AlBr_3$ complexes have been carried out using the static method with a glass membrane null-manometer. Thermodynamic characteristics of vaporization and equilibrium gas phase dissociation of the $AlBr_3{\cdot}pyz$ complex have been determined. Comprehensive theoretical studies of $(MX_3)_n{\cdot}(pyz)_m$ complexes (M = Al, Ga; X = Cl, Br, I; n = 1, 2; m = 1–3) have been carried out at the B3LYP/TZVP level of theory. Donor–acceptor bond energies were obtained taking into account reorganization energies of the fragments. Computational data indicate that the formation of $(MX_3{\cdot}pyz)_\infty$ polymers with coordination number 5 is only slightly more energetically favorable than the formation of molecular complexes of type $MX_3{\cdot}pyz$ for X = Cl, Br. It is expected that on melting $(MX_3{\cdot}pyz)_\infty$ polymers dissociate into individual $MX_3{\cdot}pyz$ molecules. This dovetails with low melting enthalpies of the $(MX_3{\cdot}pyz)_\infty$ complexes. Polymer stability decreases in the order $AlCl_3 > AlBr_3 > GaCl_3 > AlI_3 > GaBr_3 > GaI_3$. For $MI_3{\cdot}pyz$ complexes computations predict that the monomeric structure motif is more energetically favorable compared to the catena polymer. These theoretical predictions agree well with the experimentally observed monomeric complex $GaI_3{\cdot}pyz$ in the solid state. Thus, the Lewis acidity of the group 13 halides may play a decisive role in the formation of 1D polymeric networks.

Received 10th April 2013,
Accepted 11th June 2013

DOI: 10.1039/c3dt50954k

www.rsc.org/dalton

Introduction

Group 13 element trihalides are strong Lewis acids which form stable donor–acceptor complexes with nitrogen-containing bases.[1–3] Volatile group 13–15 donor–acceptor complexes are prospective single-source precursors (SSP) for the chemical vapor deposition (CVD) of binary and composite nitrides.[4,5] Volatility and the strength of the donor–acceptor bond are the two key characteristics of a successful SSP. Volatility of the solid adduct is determined by its sublimation enthalpy, which in turn depends on the structural properties of the compounds. Complexes which exhibit isolated molecules in their crystal structures have lower sublimation enthalpies and are usually more volatile than polymeric and ionic compounds.[2] Complexes with large donor–acceptor bond energies and sufficient volatility, such as the pyridine adducts $MX_3{\cdot}Py$, reveal a significant concentration in vapors even at elevated (600–800 K) temperatures.[2,6]

Usually, complexes with monodentate donors, for example $AlCl_3{\cdot}NH_2{}^tBu$,[5] are used as SSP for the synthesis of binary

[a]*Inorganic Chemistry Group, Department of Chemistry, St. Petersburg State University, University Pr. 26, Old Peterhof, St. Petersburg, 198504, Russia. E-mail: alextim@AT11692.spb.edu*
[b]*Department of Inorganic Chemistry, University of Regensburg, 93040 Regensburg, Germany. E-mail: manfred.scheer@chemie.uni-regensburg.de*

†Electronic supplementary information (ESI) available: Crystal structure information for studied complexes, results of quantum chemical computations (total energies, BSSE energies, standard entropies and enthalpies, optimized structures and *xyz* coordinates for all studied compounds obtained at the B3LYP/TZVP level of theory), summary of tensimetry experiments (26 pages). CCDC 927394–927398. For ESI and crystallographic data in CIF or other electronic format see DOI: 10.1039/c3dt50954k

13–15 compounds. For generating ternary and composite nitrides SSP should have different group 13 elements in the same molecule. This may be achieved by the introduction of the bifunctional donors LL. Complexes with LL = ethylenediamine (en), tetramethylethylenediamine (tmen) containing organometallic derivatives MR_3 adopt molecular structures $MR_3{\cdot}LL{\cdot}MR_3$,[7] but have weak donor–acceptor (DA) bonds and dissociate upon heating.[4] Both theoretical and experimental studies[2,3,8,9] show that the substitution of organometallic acceptors by group 13 element halides strongly increases the DA bond energy of complexes with monodentate donors. It is natural to assume that such a trend will hold for the complexes with bifunctional donors as well. Our previous study of group 13 metal halide complexes with en and tmen[10] showed that such complexes adopt ionic structures $[M(LL)X_2]^+[M'X_4]^-$, in which en and tmen serve as chelating bidentate ligands. It is expected that the use of non-chelating rigid bifunctional donors will be suitable for the formation of molecular mixed metal precursors.

In continuation of our studies on structures, volatility, and gas-phase stability of group 13 element halides with monodentate nitrogen-containing donors,[2] we turned our attention to complexes with rigid bifunctional donor pyrazine (pyz). Polymeric structures of $GaCl_3{\cdot}pyz$ and $GaBr_3{\cdot}pyz$ in the solid state were established in 2007 by Richards and co-workers.[11] Previous mass spectrometry and tensimetry studies of the complex formation in the $GaCl_3$-pyz system[12] confirmed the existence of the individual molecules $(GaCl_3)_2{\cdot}pyz$ and $GaCl_3{\cdot}pyz$ in the gas phase. Both complexes undergo reversibly thermal dissociation in the gas phase; $GaCl_3{\cdot}pyz$ is the dominant form in vapors, while the $(GaCl_3)_2{\cdot}pyz$ content is very low (0.2% at 383 K and only 0.05% at 673 K).[12] It is expected that the substitution of $GaCl_3$ by the stronger Lewis acid $AlBr_3$ [8] will stabilize complexes of 2 : 1 composition in vapors. To test this hypothesis, vaporization and thermal stability of $(AlBr_3)_2{\cdot}pyz$ and $AlBr_3{\cdot}pyz$ complexes have been studied by the static tensimetric method. The structures of both complexes, as well as their $GaCl_3$ analogs, and the $GaI_3{\cdot}pyz$ adduct have been determined by X-ray structural analysis. In addition, results of comparative theoretical DFT studies of $(MX_3)_n{\cdot}(pyz)_m$ (M = Al,Ga; X = Cl,Br,I; n = 1,2; m = 1–3) are also reported.

Results and discussion

I. Structural studies

Let us first consider results of structural investigation of the complexes. Expected structural types of the molecular complexes are presented in Fig. 1 (M – group 13 metal, X – halogen, L – monodentate, LL – bifunctional donor ligand). Note that the group 13 metal can adopt both tetrahedral (Fig. 1a–c) and trigonal bipyramidal environments (Fig. 1d,e). LL serves either as a terminal monodentate ligand (Fig. 1b) or as a bridging ligand with formation of distinct molecules MX_3-LL-MX_3 (Fig. 1c) or infinite polymeric chains -LL-MX_3-LL-MX_3- (Fig. 1e).

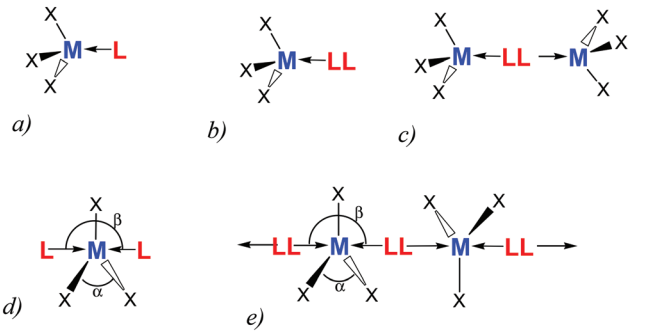

Fig. 1 Expected structural types of the molecular complexes of group 13 element halides MX_3 with monodentate (a,d) and bifunctional (b,c,e) donor ligands L and LL. Definition of α and β angles for the determination of τ values.

We have been able to grow single crystals of complexes of the bifunctional donor pyz with 2 : 1 composition $(AlBr_3)_2{\cdot}pyz$ (**1**), $(GaCl_3)_2{\cdot}pyz$ (**2**), and 1 : 1 composition $AlBr_3{\cdot}pyz$ (**3**), $GaCl_3{\cdot}pyz$ (**4**), $GaI_3{\cdot}pyz$ (**5**). Experimental details of all complexes are presented in Table S1.† We will start our discussion with structural features of the complexes with a 2 : 1 composition.

Complexes $(MX_3)_2{\cdot}pyz$. In contrast to en and tmen, which form ionic complexes $[M(LL)X_2]^+[MX_4]^-$,[10] pyrazine serves as a bridging ligand, coordinating two molecules of MX_3 with formation of molecular complexes $MX_3{\cdot}pyz{\cdot}MX_3$. **1** and **2** are isostructural, molecular structure of **1** is shown in Fig. 2, structure of **2** is available in the ESI.† In these complexes the central atom M adopts a usual tetrahedral environment with coordination number 4. However, DA bond distances in **1** and **2** (1.999 and 2.044 Å, respectively) are noticeably larger compared to M–N distances in complexes with monodentate donor Py (1.935(3) and 1.966(2) Å for $AlBr_3{\cdot}Py$ and $GaCl_3{\cdot}Py$, respectively[13]).

Complexes $MX_3{\cdot}pyz$. The molecular structures of the compounds $(AlBr_3{\cdot}pyz)_\infty$ (**3**) and $GaI_3{\cdot}pyz$ (**5**) are given in Fig. 3–5. Data for $(GaCl_3{\cdot}pyz)_\infty$ **4** are in good agreement with previously reported values by Samanamu *et al.*[11] (in their work[11] the complex was synthesized in tetrahydrofuran solution and recrystallized from diethyl ether). Note that in **3** and **4** pyrazine serves as a bridging ligand with formation of a polymeric chain in which the group 13 metal possesses the coordination number five. The halogen atoms always occupy equatorial, and the nitrogen atoms – axial positions. The MX_3 fragment remains essentially planar. Compounds **3** and **4** are isostructural and the bond distance M–N in **3** (2.133 Å) is by 0.07 Å shorter than in **4** (2.203 Å). Such a trend agrees well with the

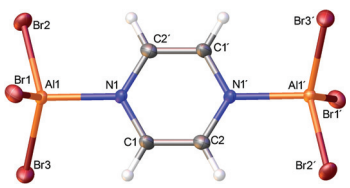

Fig. 2 Molecular structure of complex $AlBr_3{\cdot}pyz{\cdot}AlBr_3$ (**1**) in the crystal.

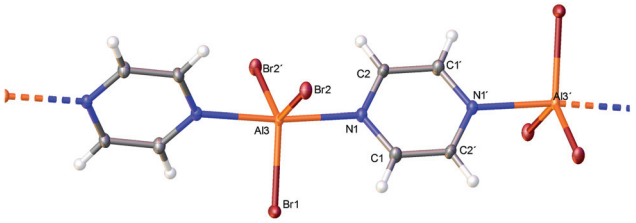

Fig. 3 Molecular structure of complex $(AlBr_3{\cdot}pyz)_\infty$ (**3**) in the crystal.

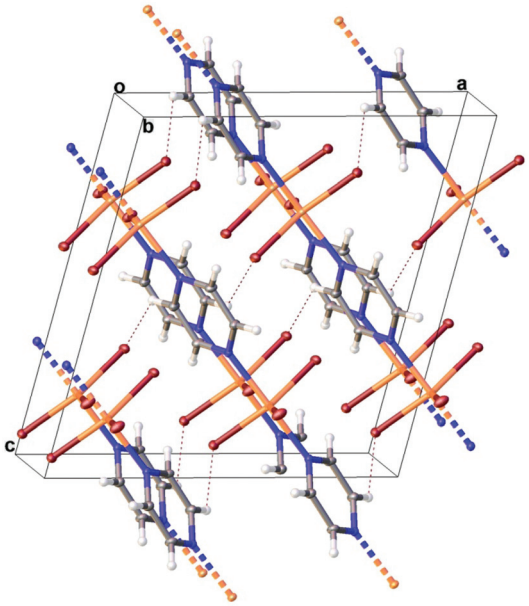

Fig. 4 Packing of the polymer chains in the crystal on the example of $(AlBr_3{\cdot}pyz)_\infty$ (**3**).

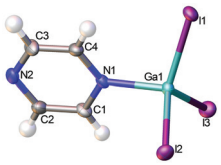

Fig. 5 Molecular structure of complex $GaI_3{\cdot}pyz$ (**5**) in the crystal.

changes of the covalent radii of Al and Ga.[14] Note that the M–N bond distances are elongated (by 0.13–0.16 Å) on going from complexes of 2 : 1 to 1 : 1 composition due to the change in the tetrahedral environment in compounds **1** and **2** to trigonal bipyramidal in **3** and **4**. The packing of the polymer chains in a crystal of **3** is shown in Fig. 4. The closest inter-polymer H···Br contacts are 3.01 and 3.12 Å.

In contrast to the polymers **3** and **4**, $GaI_3{\cdot}pyz$ (**5**) exists in the solid state only as an individual molecule $GaI_3{\cdot}pyz$ (Fig. 5), isostructural to the molecular complex $GaI_3{\cdot}Py$.[23] The Ga–N bond distance in **5** is by 0.027 Å longer than in $GaI_3{\cdot}Py$, which indicates lower donor ability of pyrazine compared to pyridine.

Coordination polymers of group 13 metal halides. Examples of coordination polymer networks based on group 13 element halides are known. An interesting 3D polymer network was recently reported for $InF_3{\cdot}4,4'bipy$.[15] The formation of 1D polymeric chains with pyrazine was reported in 2007 for gallium halides,[11] while indium and thallium trihalides prefer ladder-type one-dimensional polymers.[11,16] In the present report we show that $AlBr_3$ with pyz in a 1 : 1 stoichiometry also forms a chain polymer $(AlBr_3{\cdot}pyz)_\infty$, while $GaI_3{\cdot}pyz$ exists in the form of individual molecules. Zig-zag chain polymers with 1,3-bis-(dimethylamino)propane were previously reported for AlH_3 [17] and GaH_3.[18] Other 1D polymers include catena complexes of $AlCl_3$ and $GaCl_3$ with the O-containing bidentate donor dioxane.[19,20] Interestingly, the complex $AlCl_3{\cdot}2diox$ adopts the polymeric structure $(AlCl_3{\cdot}diox)_\infty{\cdot}diox$ with "free" dioxane solvate molecules in between the polymeric chains.[19] Major structural parameters of known 1D polymers and nitrogen-containing $MX_3{\cdot}2L$ complexes of group 13 metal halides are summarized in Table 1. The Al–N distance in **3** is in the range of the reported values for $AlX_3{\cdot}2L$ complexes with bidentate nitrogen-donor ligands (2.021–2.166 Å). In the catena polymers, as well as in **3** and **4**, the trigonal bipyramidal structure is distorted. As the criterion of structure distortion from the ideal trigonal bipyramid, the use of τ-values was proposed by Addison *et al.*[21] It is defined by the formula $\tau = (\beta - \alpha)/60$, where α, β are the largest angles in the trigonal plane and along the principal axis (Fig. 1d,e). For the perfect trigonal bipyramid the τ-value equals one, and for the perfect square pyramid the τ value equals zero. For all compounds listed in Table 1, the τ-value is larger than 0.7, indicating essentially a trigonal bipyramidal environment. Interestingly, our computed τ-values for the gas phase complexes $MX_3{\cdot}2pyz$ and $(MX_3)_2{\cdot}(pyz)_3$ are very close to one (0.96–0.99), suggesting that there is very little distortion and strain is absent in the gas phase structures (Table 1). Structural changes are virtually independent of the size of the complex: valence angles and τ-values are very similar for pyz-MX_3-pyz complexes with one trigonal bipyramidal center and for pyz-MX_3-pyz-MX_3-pyz with two trigonal bipyramidal centers. We conclude that the experimentally observed inequivalence of the X–M–X angles results from the intermolecular interactions in the solid state. The largest Cl–Ga–Cl angle in 1D polymer **4** $(GaCl_3{\cdot}pyz)_\infty$ (125.4 degrees) is close to 124.8 found in $(GaCl_3{\cdot}diox)_\infty$. The distortion of **3** (largest Br–Al–Br angle is 128.1) is more pronounced and may result from the longer Al–Br distances, which are more affected by the packing strain. Worral and coauthors[20] noted that in catena $(GaCl_3{\cdot}diox)_\infty$ the Ga–Cl distances are shorter and the Ga–O distances are significantly longer than in other compounds with coordination number 5. Our results indicate that both Ga–N and Ga–Cl bond distances in **4** are by 0.03–0.04 Å longer compared to those in the benzotriazole (Hbta) complex $GaCl_3{\cdot}2Hbta$.[30]

We conclude that all studied complexes in the solid state exist either as individual molecules (**1**, **2**, **5**) or form 1D polymers (**3**, **4**). With exception of $GaI_3{\cdot}pyz$ (**5**), in all other studied complexes pyrazine serves as a bridging ligand. Especially noteworthy is the fact that in **3** and **4** the group 13 element adopts a trigonal bipyramidal environment, with pyrazine

Table 1 Structural parameters of polymer compounds of aluminum and gallium trihalides and complexes with monodentate nitrogen-containing donors with trigonal bipyramidal geometries

Compound	R(M–N) (Å)	Max X–M–X (°)	N–M–N (°)	τ Value	Reference
$AlCl_3{\cdot}2NMe_3$	2.1580(16); 2.1662(16)	121.08(2)	178.76(5)	0.96	22
$AlCl_3{\cdot}2NHMe_2$	2.051(3); 2.073(3)	126.3(1)	176.5(1)	0.84	23
	2.051(3); 2.057(3)	124.7(1)	176.8(1)	0.87	23
	2.058(3); 2.066(3)	124.7(1)	177.6(2)	0.88	24
	2.060(3); 2.078(3)	126.3(1)	176.8(2)	0.84	24
$AlCl_3{\cdot}2morph^b$	2.064(3); 2.093(3)	129.2(1)	175.3(1)	0.77	25
$AlCl_3{\cdot}2pip^c$	2.070(5); 2.070(5)	128.6(1)	176.1(3)	0.79	26
Salpen(^{t}Bu)AlCl^d	2.031(8)^f; 1.965(7)^g	126.3(3)^h	172.3(3)^a	0.77	27
$AlCl_3{\cdot}2pyz^i$	2.182	121.0	179.9	0.98	This work
$(AlCl_3)_2{\cdot}(pyz)_3{}^i$	2.160; 2.226	120.5	179.8	0.99	This work
$(AlCl_3{\cdot}diox)_\infty{\cdot}diox$	2.016(7)^k	128.7(1)	175.3(1)^j	0.78	19
Salpen(^{t}Bu)AlBr	2.024(5)^f; 1.958(5)^g	127.3(2)^h	173.5(2)	0.77	28
	2.021(7)^f; 1.962(4)^g	126.0(2)^h	172.7(2)	0.78	28
$(AlBr_3{\cdot}pyz)_\infty$ (**3**)	2.133(2);	128.09(6)	173.13(13)	0.75	This work
$AlBr_3{\cdot}2pyz^i$	2.208	120.5	179.1	0.98	This work
$(AlBr_3)_2{\cdot}(pyz)_3{}^i$	2.182; 2.259	120.3	178.0	0.96	This work
$(AlBr_3{\cdot}diox)_\infty$	2.053(3)^k	129.8(1)	172.4(2)^j	0.71	29
$AlI_3{\cdot}2pyz^i$	2.242, 2.244	122.6	173.4	0.85	This work
$(AlI_3)_2{\cdot}(pyz)_3{}^i$	2.215; 2.230; 2.231	120.8	176.9	0.94	This work
$GaCl_3{\cdot}2Hbta^e$	2.169(2); 2.169(2)	123.3(1)	177.0(1)	0.90	30
$(GaCl_3{\cdot}pyz)_\infty$ (**4**)	2.2112(15)	125.17(12)	175.52(7)	0.84	11
$(GaCl_3{\cdot}pyz)_\infty$ (**4**)	2.203(5)	125.36(6)	175.68(17)	0.84	This work
$GaCl_3{\cdot}2pyz^i$	2.276	120.8	179.95	0.99	This work
$(GaCl_3)_2{\cdot}(pyz)_3{}^i$	2.243; 2.336	120.3	179.96	0.99	This work
$(GaCl_3{\cdot}diox)_\infty$	2.206(8)^k	124.8(1)	175.4(2)^j	0.84	20
$(GaBr_3{\cdot}pyz)_\infty$	2.262(6)	126.10(5)	174.2(3)	0.80	11
$GaBr_3{\cdot}2pyz^i$	2.326	120.6	179.7	0.99	This work
$(GaBr_3)_2{\cdot}(pyz)_3{}^i$	2.277; 2.416	120.4	179.7	0.99	This work
$GaI_3{\cdot}2pyz^i$	2.424; 2.425	120.0	178.6	0.98	This work

^{a} N–M–O angle. ^{b} Morph – morpholine. ^{c} Pip – piperidine. ^{d} Salpen – *N*,*N*′-propylenebis(3,5-di-*tert*-butylsalicylideneimine). ^{e} Hbta – benzotriazole. ^{f} Axial M–N bond distance. ^{g} Equatorial M–N bond distance. ^{h} N–Al–O angle. ^{i} Computed for the gas phase complex at the B3LYP/TZVP level of theory. ^{j} O–Al–O angle. ^{k} M–O distance.

ligands occupying the axial positions. In contrast, complex $GaCl_3{\cdot}2Py$ adopts an ionic structure $[GaCl_2Py_4]^+[GaCl_4]^-$ instead of a molecular trigonal bipyramidal adduct.[31] Such difference underlines the importance of intermolecular interactions in the solid state.

II. Computational studies

In order to get insight into the stability of the 1D polymers, quantum chemical computations have been carried out. Direct comparison between experimental and computed values for $MX_3{\cdot}pyz$ complexes of a 1 : 1 composition is not possible due to different structural environments: trigonal bipyramidal in the solid state polymer *versus* tetrahedral for the gas phase complex. In this respect, to model a polymeric chain, we optimized structures of MX_3–pyz complexes of 2 : 1, 1 : 1, 1 : 2, and 2 : 3 compositions (Fig. S6†). Structures of the considered complexes, obtained structural parameters, atomic and fragment charges, thermodynamic characteristics of the complex formation are presented in full in the ESI.† Structural parameters of the complexes are in good agreement with experimental data (Table S2†).

Optimized structures of individual complexes $MX_3{\cdot}pyz$ and $(MX_3)_2{\cdot}pyz$ reveal a tetrahedral environment at the group 13 metal. In the first complex pyrazine acts as a monodentate, and in the second – as a bridging ligand. Upon additional coordination of MX_3, the M–N distances increase by 0.037–0.045 Å, indicating weaker M–N interaction in the second complex. In the complexes of 1 : 2 and 2 : 3 composition the group 13 metal adopts a trigonal bipyramidal environment and the M–N distance is further increased by 0.135 Å. For the complex $(MX_3)_2(pyz)_3$ the M–N distances with terminal pyrazine ligands are by 0.08–0.09 Å shorter than those with the bridging pyrazine. It can be concluded that the M–N bond distance undergoes significant changes depending on the coordination environment of the group 13 atom.

In the following the thermodynamic parameters for the dissociation processes of the complexes are considered. Computed proton affinities of Py and pyz are 937 and 881 kJ mol^{-1}, in good agreement with the experimental values of 929 ± 4 and 882 ± 4 kJ mol^{-1} for Py and pyz, respectively.[32] Based on these values, Py is the stronger donor compared to pyz. The computed second proton affinity of pyz is much smaller (403 kJ mol^{-1}), which may result from electrostatic repulsion in the pyrazinium dication $HpyzH^{2+}$. Dissociation enthalpies of molecular complexes with group 13 element trihalides of 1 : 1 composition (Table 3) are considerably lower than proton affinities. Pyrazine complexes are by about 19 kJ mol^{-1} weaker bound than pyridine ones, in accordance with proton affinity trends. Aluminum trichloride forms the most stable complexes. Acceptor ability of Lewis acids decreases in the order

$AlCl_3$ > $AlBr_3$ > $GaCl_3$ > $GaBr_3$ which is in line with an increase of the DA bond distances. Stronger Lewis acids have larger values of charge transfer (equal to charge of the acceptor MX_3) and a larger negative charge on the nitrogen atom of the donor molecule (Table 4).

Another useful criterion of the complex stability in the gas phase is the value of temperature at which the equilibrium constant for the complex dissociation process equals one. It may be estimated using standard dissociation enthalpies and entropies: $T_{K=1} \approx \Delta_{diss}H^{\circ}_{298}/\Delta_{diss}S^{\circ}_{298}$. This single criterion combines both energetic and entropy factors. According to $T_{K=1}$ values, complexes of 1 : 1 composition are most stable in vapors ($T_{K=1}$ are in the range 660–940 K). The $T_{K=1}$ values for 2 : 1, 1 : 2 and 2 : 3 complexes are significantly lower due to the entropy factor. Our theoretical results are in agreement with the experimental observations of complexes with a 1 : 1 composition in vapors.[2,33]

Estimation of the donor–acceptor bond energy. In order to make a comparison between the stability of tetrahedral and trigonal bipyramidal complexes, the reorganization energy required for the pyramidalization of the acceptor MX_3 must be taken into account. Reorganization energies of group 13 metal trihalides from planar to perfectly pyramidal environment (tetrahedral XMX angle) are generally below 90 kJ mol^{-1}.[13] Since the XMX angles in DA complexes are larger than the tetrahedral ones, the reorganization energies upon complex formation are usually smaller (below 35 kJ mol^{-1} [34,35]). In the present report we computed reorganization energies for the donor and acceptor fragments and obtained values of DA bond energy (Table 4): $nE_{DA} = \Delta_{diss}E^{\circ} + kE^{reorg}(MX_3) + lE^{reorg}$-(pyz), where n – number of the DA bonds in the molecule, k, l – number of MX_3 and pyz fragments, respectively. The comparison with MX_3·Py analogs[13] shows that DA bond energies of MX_3pyz complexes are by about 25 kJ mol^{-1} smaller. These data are in good agreement with the increase of the M–N bond distances in pyz complexes compared to Py (Table 2). The formation of the DA bond with a second MX_3 molecule lowers the DA bond energy (for MX_3·pyz·MX_3 complexes by 25 kJ mol^{-1} compared to MX_3pyz). Changes in the partial charges of MX_3 fragments follow the energetic trends, suggesting that in MX_3·pyz·MX_3 two acceptors compete for the transferred charge. For complexes of 2 : 1 composition, mixed metal compounds MX_3·pyz·M′X_3 (M,M′ = Al, Ga; X = Cl, Br) have been also studied theoretically (Table S5†). Dissociation enthalpies of mixed metal (heteronuclear) complexes can be obtained from values for homonuclear complexes using a simple additive scheme.

Much lower (by 60–70 kJ mol^{-1}) DA bond energies are observed for $MX_3(pyz)_2$ complexes with a trigonal pyramidal structure. Donor atoms occupy the axial positions which are energetically less preferable. However, in this case the charge transfer to the MX_3 fragment slightly increases, since now two pyz donor molecules provide the electron density for the acceptor.

Computed DA bond energies allow us to address the question about the most preferable structure of the 1 : 1 complexes. Values of the DA bond energies, derived from the $(MX_3)_2(pyz)_3$ compound, may be taken as a first approximation to the M–N bond energies in the catena polymer $(MX_3·pyz)_\infty$. Our computations predict that the DA bond is much stronger for the individual molecule MX_3·pyz (tetrahedral environment) than in the $(MX_3·pyz)_\infty$ polymer with a trigonal bipyramidal environment. However, due to the fact that in the polymer two DA bonds are formed per one MX_3 unit, the total interaction energy slightly favors the formation of the catena polymer. The much lower reorganization energy of MX_3 in the polymer also facilitates the polymer formation. Formation of the polymeric structures in the gas phase is energetically favored by 21, 9, 11 kJ mol^{-1} for $AlCl_3$, $AlBr_3$ and $GaCl_3$ acceptors, respectively. In the case of the weaker acceptor $GaBr_3$ computations predict almost equal Ga–N interaction energies for the formation of an individual molecule $GaBr_3$·pyz and $(GaBr_3·pyz)_\infty$ polymer (the energy difference is less than 1 kJ mol^{-1}). Such small energetic differences between molecular and polymeric forms predicted for the gas phase structures imply that intermolecular interactions in the solid state can influence the preference of one or the other structural type.

A much lower Ga–N bond stability in the $GaBr_3$·pyz polymer may explain the relatively low melting point of $(GaBr_3·pyz)_\infty$ (88–90 °C[11]) compared to the isostructural compounds $(GaCl_3·pyz)_\infty$ (178–180 °C[11]) and $(AlBr_3·pyz)_\infty$ (circa 266 °C, present work). Derived from tensimetry studies melting enthalpies increase from $GaCl_3$pyz (12 ± 6 kJ mol^{-1} [12]) to $AlBr_3$pyz (64 ± 3 kJ mol^{-1}). Note that the melting points of polymers

Table 2 Comparison of experimental M–N and M–X bond distances in solid complexes with pyridine and pyrazine ligands

Compound	M–N	M–X1	M–X2	Reference
$AlBr_3$·Py	1.935(3)	2.268(1)	2.277(1), 2.280(1)	13
$AlBr_3$·pyz·$AlBr_3$ (**1**)	1.999(6)	2.2537(18)	2.267(2), 2.2463(16)	This work
$(AlBr_3·pyz)_\infty$ (**3**)	2.133(2)	2.3099(15)	2.3257(8)	This work
$GaCl_3$·Py	1.966(2)	2.1503(7)	2.1587(7), 2.1598(7)	13
$GaCl_3$·pyz·$GaCl_3$ (**2**)	2.044(7)	2.135(2)	2.147(2)	This work
$(GaCl_3·pyz)_\infty$ (**4**)[a]	2.203(5)	2.174(2)	2.1855(14)	This work
$(GaCl_3·pyz)_\infty$ (**4**)[b]	2.2112(15)	2.1758(8)	2.1822(6)	11
GaI_3·Py	2.000(4)	2.5106(6)	2.5191(7), 2.5246(6)	13
GaI_3·pyz (**5**)	2.027(6)	2.5056(7)	2.5041(9), 2.5091(9)	This work

[a] 123 K. [b] 293 K.

Table 3 Predicted standard enthalpies $\Delta_{diss}H^{\circ}_{298}$ (kJ mol^{-1}), standard entropies $\Delta_{diss}S^{\circ}_{298}$ (J mol^{-1} K^{-1}) and values of the temperatures $T_{(K=1)}$ (K), at which the equilibrium constant for the dissociation of the gaseous complex into gaseous components equals one

	X = Cl			X = Br			X = I		
Process	$\Delta_{diss}H^{\circ}_{298}$	$\Delta_{diss}S^{\circ}_{298}$	$T_{K=1}$	$\Delta_{diss}H^{\circ}_{298}$	$\Delta_{diss}S^{\circ}_{298}$	$T_{K=1}$	$\Delta_{diss}H^{\circ}_{298}$	$\Delta_{diss}S^{\circ}_{298}$	$T_{K=1}$
AlX_3·Py = AlX_3 + Py	147.6	148.4	995	137.1	151.6	904	120.3	146.4	822
AlX_3·pyz = AlX_3 + pyz	128.3	136.4	941	118.0	139.4	847	101.6	136.1	746
AlX_3·pyz·AlX_3 = 2AlX_3 + pyz	222.7	280.3	795	203.2	286.9	708	173.3	291.2	595
$AlX_3(pyz)_2$ = AlX_3 + 2pyz	161.0	291.5	541	140.0	284.3	492	108.9	295.2	369
$(AlX_3)_2(pyz)_3$ = 2AlX_3 + 3pyz	313.6	580.8	540	271.4	579.2	469	209.5	596.6	351
GaX_3·Py = GaX_3 + Py	122.0	146.7	832	108.3	149.2	726	89.0	140.7	633
GaX_3·pyz = GaX_3 + pyz	103.5	134.5	770	90.4	136.7	661	72.3	130.9	552
GaX_3·pyz·GaX_3 = 2GaX_3 + pyz	176.2	273.6	644	152.3	279.4	545	120.1	285.9	420
$GaX_3(pyz)_2$ = GaX_3 + 2pyz	127.3	282.1	451	102.7	277.3	370	70.4	268.1	262
$(GaX_3)_2(pyz)_3$ = 2GaX_3 + 3pyz	247.7	567.1	434	199.3	562.5	354	—[a]	—[a]	—[a]

[a] Structure optimization of $(GaI_3)_2(pyz)_3$ converges to two GaI_3·pyz complexes and free pyz.

Table 4 DA bond energies, E(M–N), kJ mol^{-1}, atomic charge on nitrogen atom q(N), and charge per one MX_3 unit, q(MX_3)

	X = Cl			X = Br			X = I		
Compound	E(M–N)	q(N)	$q(MX_3)$	E(M–N)	q(N)	$q(MX_3)$	E(M–N)	q(N)	$q(MX_3)$
AlX_3·Py	198.4	−0.076	−0.278	187.3	−0.090	−0.274	167.3	−0.105	−0.275
AlX_3·pyz	172.6	−0.118	−0.253	161.8	−0.131	−0.246	143.4	−0.147	−0.245
AlX_3·pyz·AlX_3	146.8	−0.100	−0.190	136.9	−0.113	−0.178	120.9	−0.129	−0.176
$AlX_3(pyz)_2$	99.1	−0.161	−0.291	88.6	−0.174	−0.277	72.6	−0.187	−0.287
$(AlX_3)_2(pyz)_3$	96.0	−0.153	−0.268	85.2	−0.170	−0.251	68.9	−0.183	−0.245
GaX_3·Py	167.0	−0.134	−0.263	152.0	−0.149	−0.255	129.6	−0.167	−0.240
GaX_3·pyz	142.3	−0.161	−0.236	128.1	−0.175	−0.224	107.4	−0.193	−0.206
GaX_3·pyz·GaX_3	118.6	−0.143	−0.175	106.2	−0.157	−0.161	88.7	−0.176	−0.144
$GaX_3(pyz)_2$	79.3	−0.185	−0.259	65.9	−0.200	−0.230	47.3	−0.212	−0.185
$(GaX_3)_2(pyz)_3$	76.8	−0.184	−0.240	63.6	−0.197	−0.210	—[a]	—[a]	—[a]

[a] Structure optimization of $(GaI_3)_2(pyz)_3$ converges to two GaI_3·pyz complexes and free pyz.

increase along with the increase of the M–N bond energy (DA bond energies are 64, 77 and 85 kJ mol^{-1} for $GaBr_3$, $GaCl_3$ and $AlBr_3$, respectively). In our opinion, this indicates a destruction of the $(MX_3$·pyz$)_\infty$ polymers upon melting.

It should be noted that according to our experimental results, GaI_3pyz (**5**) does not form a polymeric structure in the solid state (Fig. 5). Interestingly, numerous attempts on geometry optimization of $(GaI_3)_2(pyz)_3$ (starting from pyz-GaI_3-pyz-GaI_3-pyz geometry) failed due to a dissociation of the middle Ga–N bonds in course of geometry optimization. Optimization always converged to two GaI_3·pyz complexes and free pyz. This theoretical result is in excellent agreement with experimental observation of the monomeric molecular structure of **5** in the solid state. Taking the Ga–N bond energy derived from $GaI_3(pyz)_2$ as the mean Ga–N bond energy in the hypothetical gaseous polymer $(GaI_3$·pyz$)_\infty$ we conclude that the monomeric complex GaI_3·pyz is by 12 kJ mol^{-1} more stable than the polymer. The monomeric AlI_3·pyz is by 7 kJ mol^{-1} more preferable than the polymer $(AlI_3$·pyz$)_\infty$. 1-D polymer stability decreases in line with the decrease of Lewis acidity: $AlCl_3$ > $AlBr_3$ > $GaCl_3$ > AlI_3 > $GaBr_3$ > GaI_3. Thus, the Lewis acidity of group 13 halides plays a decisive role in the formation of 1D polymeric arrangement.

III. Tensimetry studies in the $AlBr_3$–pyz system

In order to obtain thermodynamic parameters for vaporization and gas phase dissociation of **1** and **3**, a series of vapor pressure–temperature measurements have been performed with the static tensimetry method with a glass membrane null-manometer. Such a technique can be used to study both heterogeneous and (after complete vaporization of the substance) homogeneous gas phase equilibria. Detailed description of the method and its application to several case studies can be found in a recent review.[2] Summary of the experiments, carried out for the $AlBr_3$–pyz system, is given in Table S6.† Since in analogy with $(GaCl_3)_2$pyz[12] it is expected that complex $(AlBr_3)_2$pyz will undergo dissociation into $AlBr_3$·pyz upon heating, vaporization and the thermal stability of individual complex $AlBr_3$·pyz was studied first.

Tensimetry studies of complex of a 1 : 1 composition. In the first two experiments, the individual complex **3**, purified by sublimation in a vacuum, was studied. Data obtained in two independent experiments 1 and 2 agree well with each other. In experiment 1, 36.2 mg of $AlBr_3$·pyz were sublimed into the system (volume 27.40 ml). Three heating–cooling cycles (up to temperature 675 K) with the heating range of about 1–2 °C per minute were performed. After heating above 674 K, very minor

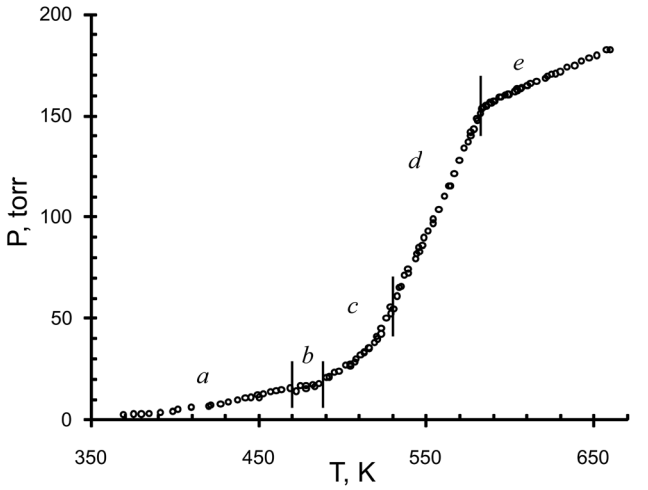

Fig. 6 Vapor pressure–temperature dependence for the $AlBr_3$·pyz complex (experiment 1). (a) Evolution of "parasitic" gas; (b) thermal expansion region; (c) sublimation of $AlBr_3$·pyz; (d) vaporization of $AlBr_3$·pyz; (e) unsaturated vapor region.

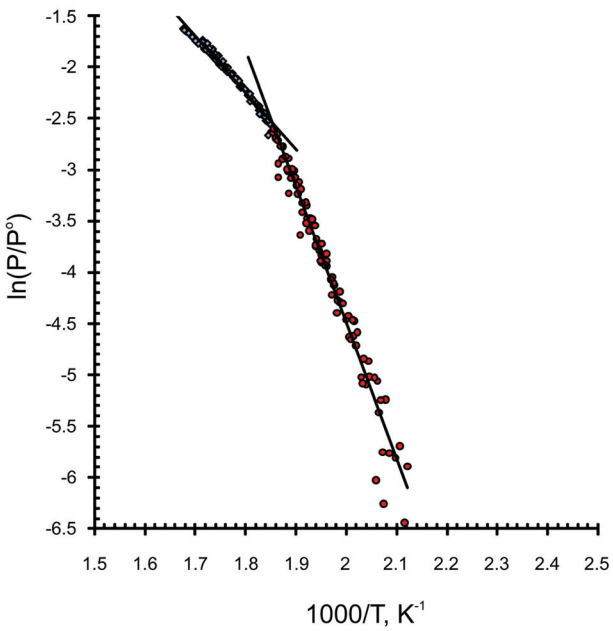

Fig. 7 $\ln(P/P^\circ) = f(1000/T)$ dependence in the saturated vapor pressure region of $AlBr_3$·pyz after the correction to the "parasitic" gas. Joint data from experiments 1 and 2. Red circles: sublimation (88 data points); blue rhombs: vaporization (80 data points).

decomposition of the organic ligand was evident as light darkening on the walls of the glass system. Measured vapor pressure–temperature dependence in experiment 1 is shown in Fig. 6 (data for the first two runs are shown). Several temperature zones have been identified.

Saturated vapor pressure range. Zone (a) corresponds to vaporization of some impurity (appearance of the so called "parasitic" gas), which undergoes thermal expansion in zone (b). This residual parasitic gas has negligible vapor pressure at room temperature, indicating that it condenses, adsorbs or chemically reacts with **3**. The low apparent vaporization enthalpy of 10 ± 2 kJ mol^{-1} (obtained from linear $\ln(P/P^\circ) = f(1/T)$ dependence in zone (a)) hints to the physisorption process. The origin of this impurity is unclear, but we must note that it was present in separately synthesized samples used in experiments 1 and 2. The molar fraction of evolved "parasitic" gas is 12% (experiment 1) or 16% (experiment 2) with respect to the amount of the introduced sample. Assuming that at high temperatures this parasitic gas is unreactive, saturated and unsaturated vapor pressures of the $AlBr_3$·pyz complex were obtained by subtraction from the total pressure the partial pressure of the evolved parasitic gas, taking into account its thermal expansion. Joint treatment of the obtained partial pressures of gaseous $AlBr_3$·pyz over solid (zone c) and liquid (zone d) $AlBr_3$·pyz allowed us to establish thermodynamic characteristics for the sublimation and vaporization processes. The plot of $\ln(P/P^\circ) = f(1/T)$ dependence is given in Fig. 7. The good agreement between the data obtained in two independent experiments 1 and 2 confirms our assumption about the inertness of the parasitic gas at elevated temperatures.

Unsaturated vapor pressure range. Zone (e) corresponds to the unsaturated vapor pressure range. In this zone, only gaseous products are present in the system. At the point of exit into the unsaturated vapor range, the estimated molecular mass of the vapors agrees well with the computed one for the monomeric molecules $AlBr_3$·pyz, indicating that it is the dominant form in vapors. Upon temperature increase, the P/T values (which are proportional to the quantity of gaseous moles in the system: $P/T = nR/V$) slightly increase, which may be attributed to a homogeneous gas phase thermal dissociation of the $AlBr_3$·pyz complex upon heating:

$$AlBr_3 \cdot pyz\ (g) = AlBr_3\ (g) + pyz\ (g) \qquad (1)$$

The good agreement between the data obtained in subsequent heating/cooling runs suggests that the true equilibrium state is achieved in the system, and no irreversible side processes occur. However, the maximal partial pressure of dissociation products is less than 10 torr (dissociation degree is lower than 6%). Low partial pressures of dissociation products lead to large errors in the determination of the equilibrium constant. Joint treatment of all obtained data in the unsaturated vapor region (experiments 1 and 2, 156 experimental points in total), taking into account dimerization of $AlBr_3$ (*cf.*[36]), allowed us to estimate the dissociation enthalpy and entropy of gaseous $AlBr_3$·pyz (Table 5). Larger uncertainty is due to the smaller dissociation degree of the complex. Nevertheless, the present experimental estimation of the dissociation enthalpy as 126 ± 14 kJ mol^{-1} within the experimental errors agrees with the theoretically computed value of 118 kJ mol^{-1} and is comparable to the experimental dissociation enthalpy for the $GaCl_3$·pyz complex (124.2 ± 2.8 kJ mol^{-1} [12]).

Experiments with excess amounts of pyz. It is expected that the introduction of the free pyz ligand should prevent complex dissociation by shifting the equilibrium (1) to the left. In order

Table 5 Summary of thermodynamic characteristics, determined in the present work

			$\ln(P/P^{o}) = -A/T + B$				
Process	T (K)	Data points	$A \times 10^{-3}$	B	T_{mean} (K)	ΔH°_{T} (kJ mol^{-1})	ΔS°_{T} (J mol^{-1} K^{-1})
$AlBr_3$·pyz(s) = $AlBr_3$·pyz (g)	470–540	88	13.24 ± 0.27	22.0 ± 0.5	505	110.1 ± 2.2	183 ± 4
$AlBr_3$·pyz(l) = $AlBr_3$·pyz (g)	540–596	80	5.57 ± 0.09	7.78 ± 0.16	568	46.3 ± 0.8	64.6 ± 1.3
$AlBr_3$·pyz(s) = $AlBr_3$·pyz (l)					540	64 ± 3[a]	118 ± 5[a]
$AlBr_3$·pyz(g) = $AlBr_3$(g) + pyz (g)	595–675	156			635	126 ± 14	128 ± 22

[a] Values obtained as difference between sublimation and vaporization processes.

to check the validity of the used model, after experiment 2, 21.3 mg of pyz were introduced into the system *via* one of the branches, after this the volume of the system decreased to 30.6 ml. Three subsequent heating–cooling runs up to the temperature of 660 K were performed (experiment 3). Decomposition of the organic ligand pyz was observed at high temperatures, and the results of the successive heating/cooling cycles are not reproducible. Therefore, only data for the first heating run were analyzed. The vapor-pressure temperature dependence is shown in Fig. 8. Zone (a) corresponds to the vaporization of an excess pyz, followed by its thermal expansion in zone (b). The exponential pressure increase in zone (c) suggests liberation of chemically bound pyz, thus, formation of a complex with excess pyz is suggested (estimated complex composition $AlBr_3$·1.5pyz). This complex completely decomposes into solid $AlBr_3$·pyz and gaseous pyz above 414 K followed by vaporization of $AlBr_3$·pyz (zone d). In the unsaturated vapor region of experiment 3 (zone e), the complex dissociation was largely suppressed suggesting that the chosen model is correct.

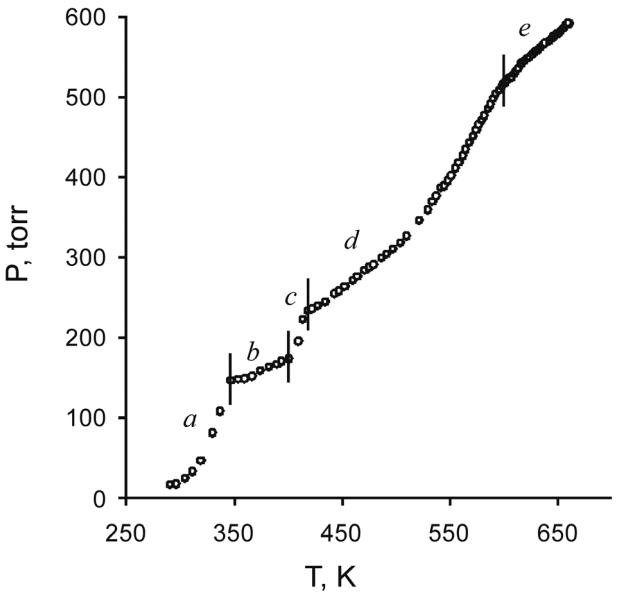

Fig. 8 Vapor pressure-temperature dependence for the $AlBr_3$·pyz complex with excess of pyz (experiment 3). (a) Saturated vapor of pyz; (b) thermal expansion region; (c) evolution of chemically bound pyz; (d) vaporization of $AlBr_3$·pyz; (e) unsaturated vapor region.

From the tensimetry study we conclude that complex $AlBr_3$·pyz vaporizes in the form of monomeric molecules $AlBr_3$·pyz, which are stable in vapors below 600 K and undergo reversible thermal dissociation into gaseous $AlBr_3$ and pyz above this temperature.

Tensimetry study of complex of 2 : 1 composition. Two tensimetry experiments have been performed, one with the separately prepared complex Al_2Br_6·pyz (experiment 4), and with a separate introduction of Al_2Br_6 and pyz into the system (experiment 5). In both experiments, a partial irreversible decomposition of the organic ligand was evidenced upon heating above 580 K (black coloring on the walls of the system), leading to irreproducibility of subsequent heating–cooling runs. However, X-ray structural analysis of a single crystal grown after experiment 4 confirmed the existence of **1** in the solid state, indicating the incompleteness of the pyrolytic process. Small partial pressures of the dissociation products and irreversible pyrolysis make it impossible to establish thermodynamic characteristics of the complex dissociation. The estimated complex dissociation degree at 575 K is 8 ± 7%. It indicates that the Al_2Br_6·pyz complex is less stable in vapors than $AlBr_3$·pyz, which is in agreement with our computational results and also in line with the order of stability found for Ga_2Cl_6·pyz and $GaCl_3$·pyz complexes.[12]

Conclusions

The formation of 1D polymers of group 13 metal halides with pyrazine is dependent on the Lewis acidity of the MX_3 moiety. While $AlBr_3$ and $GaCl_3$ form 1D polymers $(MX_3{\cdot}pyz)_\infty$, the weakest Lewis acid (GaI_3) does not afford a polymeric structure at all. GaI_3 forms the monomeric molecular complex GaI_3·pyz, which is isostructural to its pyridine analog GaI_3·py. Comprehensive theoretical studies at the B3LYP/TZVP level of theory reveal that $(MX_3{\cdot}pyz)_\infty$ polymer stability decreases in order $AlCl_3$ > $AlBr_3$ > $GaCl_3$ > AlI_3 > $GaBr_3$ > GaI_3. Upon heating the 1D polymers vaporize in the form of monomeric molecules MX_3·pyz. It is assumed that dissociation of the polymer into monomers occurs upon melting of compounds. Much lower donor properties of the second nitrogen center of the bifunctional donor pyz results in lower stability of M_2X_6·pyz complexes in the gas phase compared to MX_3·pyz complexes. An excess of MX_3 catalyzes the thermal destruction of the organic

ligand in the complexes, lowering the decomposition temperature of M_2X_6·pyz complexes by about 100 °C.

Experimental

Synthesis of adducts

Group 13 element halides were synthesized from elements and purified by multiple (not less than 4 times) resublimation in a vacuum. Due to easy hydrolysis of metal halides, all complexes have been synthesized by direct interaction of group 13 element trihalides with pyrazine in whole glass apparatus under vacuum. Analogous to the procedure described in the work,[10,12] a small excess (up to circa 10%) of the donor ligand was used for synthesis of 1 : 1 complexes MX_3·pyz. Similarly, a small excess of MX_3 was used for the synthesis of $(MX_3)_2$·pyz complexes with a 2 : 1 composition. In each case the excess component was removed by heating in a vacuum and its amount was determined. Single crystals suitable for the X-ray structural analysis have been grown by slow sublimation of the complexes in a vacuum. As typical examples, the synthesis of $(AlBr_3)_2$·pyz (**1**), $AlBr_3$·pyz (**3**), and GaI_3·pyz (**5**) complexes will be described below. Synthesis and tensimetry studies of $(GaCl_3)_2$·pyz (**2**) and $GaCl_3$·pyz (**4**) were described in ref. 12.

Synthesis of $(AlBr_3)_2$·pyz (1)

27.5 mg (0.343 mmol) of pyz was sublimated at 50 °C to 235.0 mg (0.881 mmol) of $AlBr_3$ in the vacuumed reaction vessel (Fig. S7†). The reaction started immediately upon condensation of pyz. The system was stored at 140 °C for several days. After that, an excess of $AlBr_3$ was quantitatively sublimed (80–90 °C, one day) into a special compartment and sealed off. The mass was determined (52.5 mg, 0.197 mmol). The $AlBr_3$ to pyz ratio was 1.99 ± 0.01, confirming the formation of a complex with 2 : 1 composition. Single crystals, suitable for X-ray structural analysis, were grown from the sample after the tensimetry studies (*vide supra*) by sublimation at 190–200 °C for 7 days. *m*/*z* (EI, 70 eV, 120 °C) 608–620 (M^+, <0.1%), 529–539 (M^+ − Br, <0.1), 344–350 (M^+ − $AlBr_3$, 16), 265–269 (M^+ − $AlBr_3$, −Br, 100), 185–189 ($AlBr_2^+$, 36), 106–108 ($AlBr^+$, 6), 80 (pyz^+, 41).

Synthesis of $AlBr_3$·pyz (3)

14.3 mg (0.178 mmol) of pyz was sublimated at 50 °C to 38.1 mg (0.143 mmol) of $AlBr_3$ in the vacuumed reaction vessel (Fig. S7†). The reaction started immediately upon condensation of pyz. The system was stored at 140 °C for several days. After that, an excess of pyz was sublimed (50–60 °C, 5 hours) into a special compartment, and sealed off, the mass was determined (2.7 mg, 0.034 mmol). The $AlBr_3$ to pyz ratio was 0.99 ± 0.01, in agreement with the desired 1 : 1 complex composition. Single crystals, suitable for X-ray analysis, were grown by sublimation in a vacuum at 200–220 °C for 5 days. *m*/*z* (EI, 70 eV, 120 °C) 344–350 (M^+, 7.4%), 265–269 (M^+ − Br, 90), 185–189 ($AlBr_2^+$, 35), 106–108 ($AlBr^+$, 8), 80 (pyz^+, 100).

Synthesis of GaI_3·pyz (5)

66.7 mg (0.833 mmol) of pyz was sublimated at 50 °C to 370.5 mg (0.823 mmol) of GaI_3 in the vacuumed reaction vessel (Fig. S7†). The reaction started immediately upon condensation of pyz. The system was stored at 100 °C for several days, after that the temperature was raised to 140–150 °C. Single crystals, suitable for X-ray structural analysis, were grown by sublimation in a vacuum at 200–220 °C for 5 days. *m*/*z* (EI, 70 eV, 120 °C) 530–532 (M^+, 0.02%), 403–405 (M^+ − I, 0.8), 323–325 (GaI_2^+, 22.9), 196–198 (GaI^+, 9.3), 80 (pyz^+, 100).

X-ray structure analysis of the complexes

The crystal structure analyses were performed on an Oxford Diffraction Gemini R Ultra CCD. Either semi-empirical[37] or analytical absorption corrections from crystal faces[38] were applied. The structures were solved by direct and charge-flipping methods, respectively. Thereby the programs SIR-97[39] and Superflip[40] were employed. Full matrix least-squares refinements on F^2 in SHELXL-97 were carried out.[41] The hydrogen coordinates were partially refined. All pictures were created with Olex.[2,42]

Only one very large crystal of **2** could be obtained, which had to be broken. This procedure led to split reflections and caused the relatively large quality factors. CCDC-927394, -927395, -927396, -927397 and -927398, contain the supplementary crystallographic data for this paper.

Quantum chemical computations

These were performed using DFT hybrid functional B3LYP[43] in conjunction with the triple zeta quality basis set with polarization functions. Ahlrich's all electron TZVP basis set[44a] was used for Al, Ga, C, N, Cl, Br, effective core potential def2-TZVP basis set[44b,c] was used for I, standard 6-311G** basis set[44d] was used for H. The B3LYP method has been successfully applied for the complexes of group 13 metal halides with ammonia[8] and provided good agreement with high temperature experimental data. Structures of all compounds were fully optimized and verified to be minima on their respective potential energy surfaces (PES). GAUSSIAN 03 program package[45] was used throughout. Basis set superposition error (BSSE) was estimated by the counterpoise method[46] realized in Gaussian03. BSSE was found to be less than 8 kJ mol^{-1} per donor–acceptor bond (Table S4, ESI†). In all cases the introduction of the BSSE correction does not change the order of the acceptor ability of MX_3. Given the fact that the counterpoise method generally overestimates BSSE,[46c] in the following discussion we will use reaction energies, uncorrected for BSSE.

Acknowledgements

This work was supported by St. Petersburg State University research grant 12.37.139.2011. A.Y.T. is grateful to the Alexander von Humboldt Foundation for re-invitation fellowship. Excellent service of Computer cluster of St. Petersburg State University is gratefully acknowledged.

References

1 E. N. Guryanova, I. P. Goldshtein and I. P. Romm, *Donor–Acceptor Bond*, John Wiley and Sons, New York, Toronto, 1975.
2 E. I. Davydova, T. N. Sevastianova, A. V. Suvorov and A. Y. Timoshkin, *Coord. Chem. Rev.*, 2010, **254**, 2031.
3 N. N. Greenwood and A. Earnshaw, *Chemistry of the elements*, Elsevier, Oxford, 2nd edn, 1997.
4 A. C. Jones and P. O'Brien, *CVD of Compound Semiconductors. Precursor Synthesis, Development and Applications*, VCH, Weinheim, Germany, 1997.
5 O.-S. Joo, K.-D. Jung, S.-H. Cho, J.-H. Kyoung, C.-K. Ahn, S.-C. Choi, Y. Dong, H. Yun and S.-H. Han, *Chem. Vap. Deposition*, 2002, **8**, 273.
6 (*a*) A. Y. Timoshkin, A. V. Suvorov and A. D. Misharev, *Russ. J. Gen. Chem.*, 2002, **72**, 1874; (*b*) A. Y. Timoshkin, A. A. Grigoriev and A. V. Suvorov, *Zh. Obshch. Khim.*, 1995, **65**, 1634.
7 (*a*) D. O'Hare, J. S. Foord, T. C. M. Page and T. J. Whitaker, *J. Chem. Soc., Chem. Commun.*, 1991, 1445; (*b*) D. W. Goebel, J. L. Hencher and J. P. Oliver, *Organometallics*, 1983, **2**, 746; (*c*) J. J. Byers, W. T. Pennington and G. H. Robinson, *Acta Crystallogr., Sect. C: Cryst. Struct. Commun.*, 1992, **48**, 2023; (*d*) R. B. Hallock, W. E. Hunter, J. L. Atwood and O. T. Beachley Jr., *Organometallics*, 1985, **4**, 547; (*e*) J. L. Atwood, S. G. Bott, F. M. Elms, C. Jones and C. L. Raston, *Inorg. Chem.*, 1991, **30**, 3792; (*f*) H.-E. Ting, W. H. Watson and H. C. Kelly, *Inorg. Chem.*, 1972, **11**, 374.
8 A. Y. Timoshkin, A. V. Suvorov, H. F. Bettinger and H. F. Schaefer, *J. Am. Chem. Soc.*, 1999, **121**, 5687.
9 (*a*) J. R. Creighton and G. T. Wang, *J. Phys. Chem. A*, 2005, **109**, 133; (*b*) V. I. Trusov, A. V. Suvorov and R. N. Abakumova, *Zh. Neorg. Khim.*, 1975, **20**, 501.
10 C. Trinh, M. Bodensteiner, A. Virovets, E. Peresypkina, M. Scheer, S. M. Matveev and A. Y. Timoshkin, *Polyhedron*, 2010, **29**, 414.
11 C. R. Samanamu, P. M. Lococo and A. F. Richards, *Inorg. Chim. Acta*, 2007, **360**, 4037.
12 A. Y. Timoshkin, E. A. Berezovskaya, A. V. Suvorov and A. D. Misharev, *Russ. J. Gen. Chem.*, 2005, **75**, 1173.
13 A. Y. Timoshkin, M. Bodensteiner, T. N. Sevastianova, A. S. Lisovenko, E. I. Davydova, M. Scheer, C. Graßl and A. V. Butlak, *Inorg. Chem.*, 2012, **51**, 11602.
14 J. E. Huheey, E. A. Keiter and R. L. Keiter, *Inorganic Chemistry: Principles of Structure and Reactivity*, HarperCollins, New York, 4th edn, 1993.
15 S. P. Petrosyants and A. B. Ilyukhin, *Russ. J. Inorg. Chem.*, 2010, **55**, 30.
16 C. R. Samanamu and A. F. Richards, *Polyhedron*, 2007, **26**, 923.
17 J. L. Atwood, F. R. Bennett, C. Jones, G. A. Koutsantonis, C. L. Raston and K. D. Robinson, *J. Chem. Soc., Chem. Commun.*, 1992, 541.
18 J. Lorberth, R. Dorn, S. Wocadlo, W. Massa, E. O. Göbel, T. Marschner, H. Protzmann, O. Zsebök and W. Stolz, *Adv. Mater.*, 1992, **4**, 576.
19 A. Boardman, R. W. H. Small and I. J. Worral, *Acta Crystallogr., Sect. C: Cryst. Struct. Commun.*, 1983, **39**, 433.
20 A. Boardman, S. E. Jeffs, R. W. H. Small and I. J. Worral, *Inorg. Chim. Acta*, 1984, **87**, L27.
21 A. W. Addison, T. N. Rao, J. Reedijk, J. van Rijn and G. C. Verschoor, *J. Chem. Soc., Dalton Trans.*, 1984, 1349.
22 T. Gelbrich, U. Dümichen and J. Sieler, *Acta Crystallogr., Sect. C: Cryst. Struct. Commun.*, 1999, **55**, 1797.
23 A. Ahmed, W. Schwarz, J. Weidlein and H. Hess, *Z. Anorg. Allg. Chem.*, 1977, **434**, 207.
24 E. B. Lobkovskii, I. I. Korobov and K. N. Semenenko, *J. Struct. Chem.*, 1979, **19**, 908.
25 G. Müller and C. Krüger, *Acta Crystallogr., Sect. C: Cryst. Struct. Commun.*, 1984, **40**, 628.
26 L. M. Engelhardt, P. C. Junk, C. L. Raston, B. W. Skelton and A. H. White, *J. Chem. Soc., Dalton Trans.*, 1996, 3297.
27 M.-A. Munoz-Hernandez, T. S. Keizer, P. Wie, S. Parkin and D. A. Atwood, *Inorg. Chem.*, 2001, **40**, 6782.
28 A. Mitra, L. J. DePue, S. Parkin and D. A. Atwood, *J. Am. Chem. Soc.*, 2006, **128**, 1147.
29 L. Jakobsmeier, I. Krossing, H. Nöth and M. J. H. Schmidt, *Z. Naturforsch., B: Chem. Sci.*, 1996, **51**, 1117.
30 S. Zanias, C. P. Raptopoulou, A. Terzis and T. F. Zafiropoulos, *Inorg. Chem. Commun.*, 1999, **2**, 48.
31 J. Sinclair, R. W. H. Small and I. J. Worrall, *Acta Crystallogr., Sect. B: Struct. Sci.*, 1981, **37**, 1290.
32 M. Meot-Ner, *J. Am. Chem. Soc.*, 1979, **101**, 2396.
33 T. N. Sevast'yanova and A. V. Suvorov, *Russ. J. Coord. Chem.*, 1999, **25**, 679.
34 A. S. Lisovenko and A. Y. Timoshkin, *Inorg. Chem.*, 2010, **49**, 10357.
35 A. Y. Timoshkin, E. I. Davydova, T. N. Sevastianova, A. V. Suvorov and H. F. Schaefer, *Int. J. Quantum Chem.*, 2002, **88**, 436.
36 A. S. Malkova, C. Sci. Dissertation, Lomonosov Moskow State University, 1969.
37 *Agilent Technologies, CrysAlisPro Software system, different versions 2006–2011*, Agilent Technologies UK Ltd, Oxford, UK.
38 R. C. Clark and J. S. Reid, *Acta Crystallogr., Sect. A: Found. Crystallogr.*, 1995, **51**, 887.
39 A. Altomare, M. C. Burla, M. Camalli, G. L. Cascarano, C. Giacovazzo, A. Guagliardi, A. G. G. Moliterni, G. Polidori and R. Spagna, *J. Appl. Crystallogr.*, 1999, **32**, 115.
40 L. Palatinus and G. Chapuis, *J. Appl. Crystallogr.*, 2007, **40**, 786.
41 G. M. Sheldrick, *Acta Crystallogr., Sect. A: Found. Crystallogr.*, 2008, **64**, 112.
42 O. V. Dolomanov, L. J. Bourhis, R. J. Gildea, J. A. K. Howard and H. Puschmann, *J. Appl. Crystallogr.*, 2009, **42**, 339.
43 (*a*) A. D. Becke, *J. Chem. Phys.*, 1993, **98**, 5648; (*b*) C. Lee, W. Yang and R. G. Parr, *Phys. Rev. B: Condens. Matter Mater. Phys.*, 1988, **37**, 785.
44 (*a*) A. Schafer, C. Huber and R. Ahlrichs, *J. Chem. Phys.*, 1994, **100**, 5829; (*b*) K. A. Peterson, D. Figgen, E. Goll, H. Stoll and M. Dolg, *J. Chem. Phys.*, 2003, **119**, 11113;

(*c*) F. Weigend and R. Ahlrichs, *Phys. Chem. Chem. Phys.*, 2005, **7**, 3297; (*d*) R. Krishnan, J. S. Binkley, R. Seeger and J. A. Pople, *J. Chem. Phys.*, 1980, **72**, 650.

45 M. J. Frisch, G. W. Trucks, H. B. Schlegel, G. E. Scuseria, M. A. Robb, J. R. Cheeseman, J. A. Montgomery Jr., T. Vreven, K. N. Kudin, J. C. Burant, J. M. Millam, S. S. Iyengar, J. Tomasi, V. Barone, B. Mennucci, M. Cossi, G. Scalmani, N. Rega, G. A. Petersson, H. Nakatsuji, M. Hada, M. Ehara, K. Toyota, R. Fukuda, J. Hasegawa, M. Ishida, T. Nakajima, Y. Honda, O. Kitao, H. Nakai, M. Klene, X. Li, J. E. Knox, H. P. Hratchian, J. B. Cross, C. Adamo, J. Jaramillo, R. Gomperts, R. E. Stratmann, O. Yazyev, A. J. Austin, R. Cammi, C. Pomelli, J. W. Ochterski, P. Y. Ayala, K. Morokuma, G. A. Voth, P. Salvador, J. J. Dannenberg, V. G. Zakrzewski, S. Dapprich, A. D. Daniels, M. C. Strain, O. Farkas, D. K. Malick, A. D. Rabuck, K. Raghavachari, J. B. Foresman, J. V. Ortiz, Q. Cui, A. G. Baboul, S. Clifford, J. Cioslowski, B. B. Stefanov, G. Liu, A. Liashenko, P. Piskorz, I. Komaromi, R. L. Martin, D. J. Fox, T. Keith, M. A. Al-Laham, C. Y. Peng, A. Nanayakkara, M. Challacombe, P. M. W. Gill, B. Johnson, W. Chen, M. W. Wong, C. Gonzalez and J. A. Pople, *GAUSSIAN 03 (Revision B.05)*, Gaussian Inc., Pittsburgh, PA, 2003.

46 (*a*) S. F. Boys and F. Bernardi, *Mol. Phys.*, 1970, **19**, 553; (*b*) S. Simon, M. Duran and J. J. Dannenberg, *J. Chem. Phys.*, 1996, **105**, 11024; (*c*) T. Clark, *A Handbook of Computational Chemistry*, Wiley, New York, 1985.